

Profiling N-Type Dopants in Silicon

Miloš Hovorka¹, Filip Mika¹, Petr Mikulík² and Luděk Frank¹

¹*Institute of Scientific Instruments of the ASCR, v.v.i., Kralovopolska 147, CZ-612 64 Brno, Czech Republic*

²*Faculty of Science, Masaryk University, Kotlarska 2, CZ-611 37 Brno, Czech Republic*

Various doped n-type structures (dopant concentration between $1.5 \times 10^{16} \text{ cm}^{-3}$ and $1.5 \times 10^{19} \text{ cm}^{-3}$) on a lightly doped p-type silicon substrate (doped to $1.9 \times 10^{15} \text{ cm}^{-3}$) have been examined by a photoemission electron microscope equipped with a high-pass energy filter and by an ultra-high vacuum scanning low energy electron microscope. High contrast has been observed between the n-type areas and the p-type substrate and its monotone dependency on the doping level of structures has been manifested. The relation between the energy spectra of photoelectrons and the doping level has been studied, too. The scanning electron microscope images obtained with the landing energy of the primary beam in the low keV range exhibit contrasts similar to those appearing in the full threshold photoemission micrographs.
[doi:10.2320/matertrans.MC200910]

(Received July 27, 2009; Accepted October 28, 2009; Published December 9, 2009)

Keywords: silicon, dopant contrast, photoemission electron microscopy, scanning electron microscopy

1. Introduction

The semiconductor industry needs suitable observation methods with high spatial resolution and sensitivity to the dopant level. They are needed to control semiconductor structures in production and to optimize the process plan. There are multiple methods used for such characterization (SSRM, SCM, TEM, SIMS, etc.), showing specific advantages and drawbacks when compared to each other.¹⁾ Among the dopant profiling techniques the scanning electron microscopy (SEM) has become a well established method exhibiting high spatial resolution as well as high sensitivity to the dopant concentration.²⁻⁴⁾ Quantitative two-dimensional dopant mapping using energy-filtered secondary electron (SE) imaging has been demonstrated with the SEM. When measuring the shift in the SE energy spectra across the p-n junction, more accurate data are obtained than what mere SE yields from selected areas provide.³⁾ There are still some open questions as regards the origin of the contrast between the doped structures, which complicates employing the SEM as a quantitative tool in the dopant profiling. The presence of hydrocarbons and oxide contamination layers on the sample surface influences the contrast behaviour significantly. Several mechanisms can contribute to the contrast creation, including the built-in voltage across the p-n junction, the surface states, local differences in the electron mean free path, the dynamic charging effect, the carbon layer creating metal-to-semiconductor contact, etc.⁵⁾

Photoemission electron microscopy (PEEM) with its simple mechanism of hot electron generation is a surface-sensitive alternative to the SEM imaging with plenty of background signals. PEEM can provide high sensitivity to the dopant concentration and is capable of imaging surfaces under various conditions. This method has already been successfully applied in the imaging and characterization of doped silicon structures,⁶⁻⁸⁾ hence indicating its applicability as an analytical tool in dopant profiling. PEEM equipped with an energy filter not only compares the local photoyields but advances the method a step forward to acquisition of the energy spectra from differently doped areas. It is possible to image the doped areas on very high contrast levels⁹⁾ when

only collecting photoelectrons of chosen energies, which is particularly useful in the threshold imaging, and to gain more reliable information about local differences in the photo threshold and surface status. Factors similar to those inherent to SEM can contribute to the contrast mechanism and the presence of contamination layers on the surface modifies the surface properties and emissivity of photoelectrons.

Experimental data for differently doped p-type areas on n-type substrate exist both from PEEM and SEM under various surface conditions. Contrast of differently doped p-type patterns has been found to be significantly dependent on the dopant concentration and the surface conditions. However, a similar data set for n-type patterns on p-type substrate seems missing. The aim of the present paper is to fill this gap.

2. Experiment

This report focuses on differently doped planar n-type structures on a p-type substrate, etched in HF prior to loading to the microscope in order to remove the native oxide layer. The sample design allowed comparison of different doping levels in one micrograph frame and therefore under identical surface conditions and treatment history. The laterally resolved photoemission threshold and X-ray spectroscopies provided information about the edge of the valence band and the Si 2p core-level for differently doped areas and the substrate. N-type structures were also imaged in a scanning electron microscope with the landing energy of the primary beam in the low range of keV.

2.1 Experimental setup

The photoemission measurements were done at the ANKA synchrotron (Karlsruhe, Germany) at the WERA beamline dedicated to soft X-ray spectroscopy and microscopy. The PEEM microscope is located inside a UHV chamber (operating pressure of about 10^{-10} mbar) and equipped with an imaging energy filter of the retarding field type¹⁰⁾ with the nominal energy resolution of about 90 meV. The filter, located in front of the multichannel plate, acts as a high-pass filter for the full image. When grounding the sample and biasing the retarding grid of the energy filter, only photo-

electrons of kinetic energy higher than the corresponding threshold can pass through to be detected. The same effect can be attained when applying a voltage to the sample relatively to the retarding grid held at an adjusted potential. The signal is amplified by the multichannel plate, imaged onto a fluorescent screen and recorded by a CCD camera.

A high-pressure mercury lamp served as the photon source for the threshold spectroscopy, with the main spectral line at 4.9 eV of a width of approximately 200 meV. The synchrotron source of X-ray radiation with energy of 220 eV (photon energy spread of about 137 meV) probed the Si 2p core-level. The angle between the surface normal and the incoming beam was 65° and the spot size was approximately 0.8 mm horizontally and 0.4 mm vertically.

The SEM data were taken by an ultra-high vacuum scanning low energy electron microscope (SLEEM) of in-house design, with the operating pressure below 10⁻⁹ mbar. The device is equipped with an all-electrostatic electron column employing a Schottky emitter as the electron source, and incorporating the cathode lens. The impact energy of the primary electron beam on the sample surface can be tuned from tens of keV to the units of eV or even fractions of eV, keeping the lateral resolution nominally in a few tens of nm. The landing energy of electrons is governed by the cathode lens, being determined by the difference between the primary beam energy and the sample bias.¹¹⁾ The collected signal consists of a mixture of backscattered (BSE) and secondary electrons the ratio of which varies with the landing energy because of the cathode lens geometry. The emitted SE and BSE, accelerated in the cathode lens field, are detected by a bored YAG (yttrium-aluminium garnet) single crystal scintillator disc and the resulted light signal is amplified by a photomultiplier.

2.2 Specimens

We prepared planar doped silicon structures suitable for microscopes equipped with the cathode lens. Lightly to heavily phosphorus doped n-type areas with the doping concentration varying from 1.5 × 10¹⁶ cm⁻³ (N16) to 1.5 × 10¹⁹ cm⁻³ (N19) were created in the p-type Si (100) substrate boron doped to 1.9 × 10¹⁵ cm⁻³ (P15). The periodic structure of doped patterns consists of stripes with nominal width and spacing of 25 μm and length of 2000 μm, and of squares of 40, 20, and 5 μm in size. Two photolithography masks were designed for 100 mm silicon wafer substrates.

The preparation incorporated multiple technological steps and was performed in the clean room laboratory at the Masaryk University (Brno, Czech Republic) and in the ON Semiconductor Czech Republic factory (Roznov pod Radhostem). The first step was to create markers in the substrate at locations defined by the first mask which were subsequently used for alignment of the second mask for differently doped patterns. These markers were etched in the substrate depth with a mixture of HF, HNO₃, CH₃COOH through openings in a thick oxide layer which was removed afterwards. Then four processing steps followed comprising of a photolithography process producing the desired structure layout into a protective photoresist layer, a 60 keV ion implantation of the requested dopant dose and cleaning of the wafer. Finally the wafers were annealed at 1100°C to

obtain the desired dopant concentration profile, which was reasonably constant up to the depth of 400 nm. The profiles were verified by the spreading resistance profiling in the ON Semiconductor Czech Republic.

Prior to loading to the observation chamber the samples were etched in 5% HF (PEEM data) or in buffered HF (SEM data) to remove the native oxide layer. Still, during the loading of the sample and obtaining high vacuum, the surfaces were likely to become covered with an ultrathin oxide layer.

3. Results and Discussion

The threshold PEEM micrographs for various retarding voltages (V_r) applied to the (chemically etched) sample are shown in Fig. 1. There are visible differently doped n-type squares embedded into the lightly doped p-type substrate (P15). The square sides are 40, 20, and 5 μm and their dopant concentration varies from 1.5 × 10¹⁶ cm⁻³ (N16) to 1.5 × 10¹⁹ cm⁻³ (N19). In the full photoemission images (see the frames labeled -1.0 V and -0.5 V), when all photoelectrons are collected for the detection, there is a clear, dopant-concentration-dependent contrast observed between the patterns and the substrate. A higher dopant concentration corresponds to a stronger contrast and it is possible to quantify the doping levels in n-type structures on the basis of their photoyields. In the full photoemission images the lightly doped n-type areas can be distinguished with rather weak contrast. This behaviour differs from previous observations of samples covered with contamination layers, i.e. samples exposed to the atmosphere for a longer time, exhibiting a quite weak full photoemission contrast for all doping levels.⁹⁾

In Fig. 2 the doping level dependency of contrast C between the n-type patterns and the substrate is plotted for the full photoemission images. The contrast is defined as $C = (S_p - S_n)/S_n$, where $S_{p,n}$ means the averaged image signal in the respective areas. The monotone tendency of the plot indicates a proportional decrease of the photoyield of the n-type area with the increasing doping level. This finding makes the pattern/substrate contrast suitable for quantitative dopant profiling.

Figure 1 further shows development in the contrast between the doped areas when the retarding voltage is increased and only photoelectrons of higher kinetic energies are detected. The lightly doped areas (N16, N17) invert their contrasts with respect to the substrate and start appearing brighter (see the frames labeled +0.1 V and +0.25 V). The bright rims around the (still dark) heavily doped areas are connected with electron-optical deflections of the emitted electron flux with lateral fields across the p-n junction.¹²⁾ Around +0.45 V the contrast inverts for all n-type areas and it is again possible to distinguish between differently doped areas according to their strong contrast differences. Moreover, the contrast between the lightly doped n-type patterns and the p-type substrate is significantly enhanced with respect to that for the full photoemission. For the fast photoelectrons the inverted contrast between patterns and substrate reaches tens of percents. Finally, let us notice the increased signal level in N18 and N19 squares for the frames labeled +0.45 V and +0.8 V (see below).

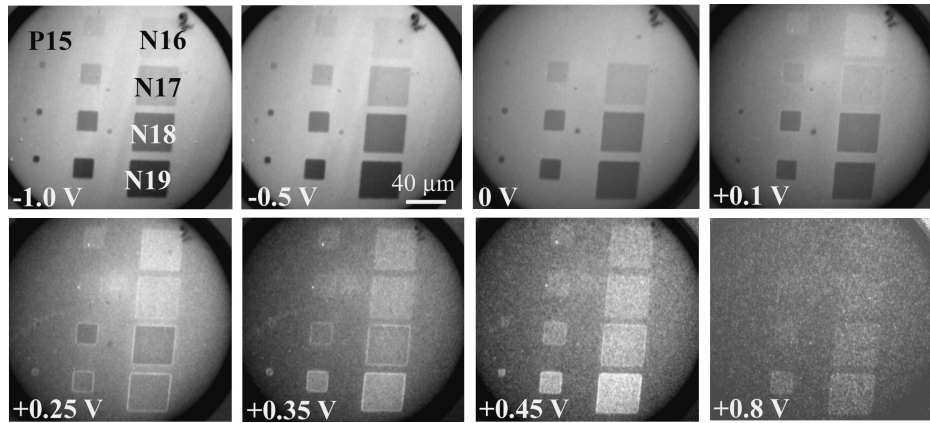


Fig. 1 PEEM micrographs taken under mercury lamp illumination for various retarding voltages (indicated in the left bottom corner of the micrographs) applied on the sample. The doping level in n-type squares varies from $1.5 \times 10^{16} \text{ cm}^{-3}$ (N16) to $1.5 \times 10^{19} \text{ cm}^{-3}$ (N19) while the p-type substrate is doped to $1.9 \times 10^{15} \text{ cm}^{-3}$ (P15). The negative retarding voltages correspond to the full photoemission imaging while with increasing voltage the slowest photoelectrons are filtered off.

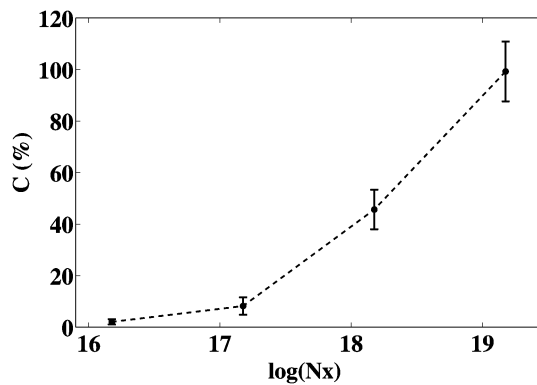


Fig. 2 Contrast C between the n-type patterns and the p-type substrate as a function of the doping level N_x in the n-type areas when all photoelectrons emitted under mercury lamp illumination are detected.

The energy spectra obtained by numerical differentiation from the measured integrated forms extracted from the images by area averaging of signals are shown in Fig. 3. The n-type spectra are generally shifted to the right relatively to the p-type spectrum of the substrate, thus to higher kinetic energies of photoelectrons. In agreement with the threshold photoemission micrographs these data exhibit clear dependency on the dopant concentration. The height of the spectra and also the total photoemission (i.e. the peak area) from n-type structures decrease with the increasing doping level but the shift between p- and n-type spectra remains around 25 meV along the full dopant scale. The shoulder of the spectral peak (see the arrow in Fig. 3) appearing for the heavily doped n-type patterns at the higher kinetic energy side could be attributed to the emission from the conduction band. In the +0.45 V and +0.8 V frames in Fig. 1 this is also visible owing to the increased signal level of two lowest squares.

In Fig. 4 one can see the core-level Si 2p photoemission spectra for the heavily doped n-type areas N18, N19 and the lightly doped p-type substrate P15. The energy of the X-ray photons was 220 eV. In the spectra the increasing retarding voltage corresponds to a decreasing binding energy of detected photoelectrons. The spectra are primarily composed

of two Si 2p partner lines, namely Si 2p_{1/2} (the peak at around 115.5 V) and Si 2p_{3/2} (the peak at around 116.1 V). They are likely to also comprise some small contributions from the intermediate-oxidation states (Si¹⁺ to Si³⁺) and the SiO₂ state (see the broad region at the higher binding energies), corresponding to the nearly oxide free surface of the HF etched sample (see e.g. Himpsel *et al.*¹³). The n-type spectra are shifted to higher binding energies than the p-type substrate spectrum and their shift is dependent on the doping level of the patterns. The shift between the N19 and the P15 spectra amounts to about 120 meV while that between N18 and P15 is about 60 meV. Thus, the spectrum shift is proportional to the dopant concentration and represents a dominating contrast source. Here we suppose that the detection efficiency of the PEEM assembly is only negligibly different for both p- and n-type spectra mutually shifted by a fraction of eV. Consequently, when passing with the energy filter across the peak region, the pattern/substrate contrast inverts in the micrographs obtained via differentiation of the measured signal from the filter. Let us underline that contrary to the micrographs in Fig. 1 taken with a high-pass filter, the images in Fig. 4 are effectively taken with a band-pass filter. In the micrograph labeled 116 V in Fig. 4, the 40 and 20 μm squares of both N18 and N19 areas are marked by white frames. The N17 and N16 patterns have not been resolved in the core-level photoemission at all.

When summarizing the main results one can see that for the threshold photoemission the main source of the pattern/substrate contrast is the spectrum height, i.e. the total photoyield (lower for the n-type). The difference in position of p- and n-type spectra in the energy scale is dopant concentration independent but still sufficient for the contrast inversion in fast photoelectron images. On the contrary, for the 2p photoemission the contrast is owing to the doping-level-proportional spectrum shift. The important fact is that in the two spectroscopy types, the spectrum shifts are of mutually opposite directions — in the threshold spectroscopy the n-type spectrum is shifted to higher kinetic energies of photoelectrons while in the 2p core-level spectroscopy the n-type spectrum is on the left, i.e. on the lower kinetic energy side.

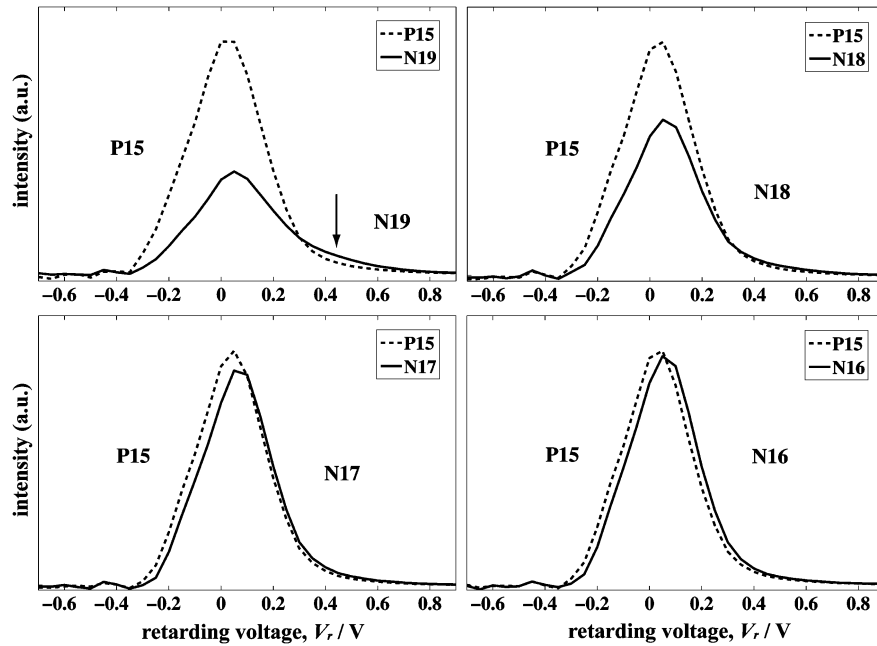


Fig. 3 Threshold energy spectra for the differently doped n-type patterns (N16 to N19) and the lightly doped p-type substrate (P15) obtained for the mercury lamp illumination.

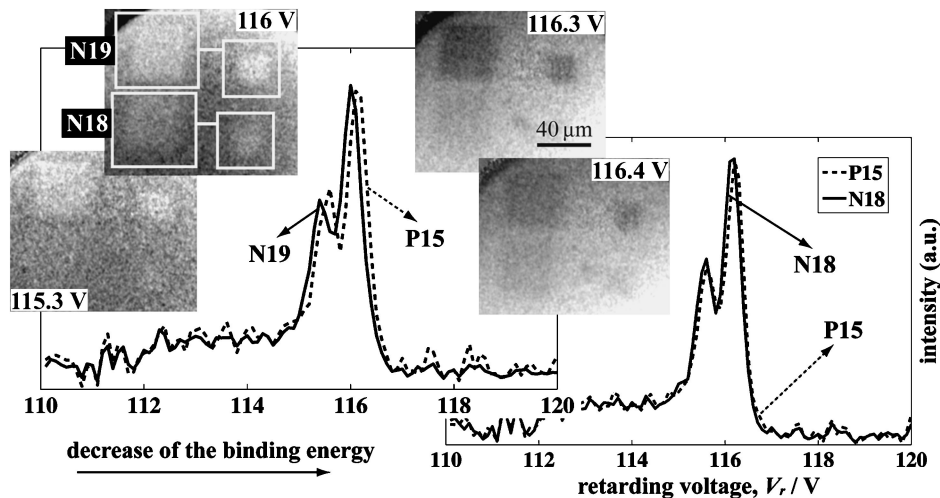


Fig. 4 Core-level Si 2p energy spectra for n-type patterns N18 and N19 and p-type substrate (P15) obtained for X-ray irradiation with the photon energy of 220 eV. The micrographs obtained via differentiation of the measured signal from the filter are shown for several retarding voltages.

Several factors can contribute to the contrast generation. The shift between the core-level spectra of the heavily doped n-type and the lightly doped p-type is rather small, albeit dopant-density-dependent. Should the built-in voltage across the p-n junction of silicon structures dominate, a much larger shift (about 0.8 eV) between the spectra would appear. However, HF-treated silicon surfaces have been shown to still exhibit some Fermi level pinning caused by surface states.¹⁴⁾ The subsurface band bending leads to a significant reduction in the shifts between n- and p-type spectra. Another factor is the surface sensitivity determined by the escape depth of photoelectrons, and the band bending can also be induced by X-ray radiation leading to some subsurface positive charging, confirmed for the HF-treated silicon surfaces.¹⁵⁾

Images obtained in the SLEEM apparatus on the chemically etched sample are presented in Fig. 5 showing the differently doped n-type stripes. The primary beam energy was 6 keV and the landing energy was determined by the sample bias applied. For the landing energy of 4 keV there is only a weak signal available from the doped stripes. Then the signal increases with decreasing landing energy and at about 2.5 keV the contrast between n-type stripes and p-type substrate becomes distinct and dependent on the dopant concentration similarly as for the full threshold photoemission in the PEEM. The n-type patterns are again darker than the p-type substrate and dependency of the contrast on the doping level is clearly pronounced in spite of some signal inhomogeneity across the field of view caused by the detection system, which complicates quantification of the

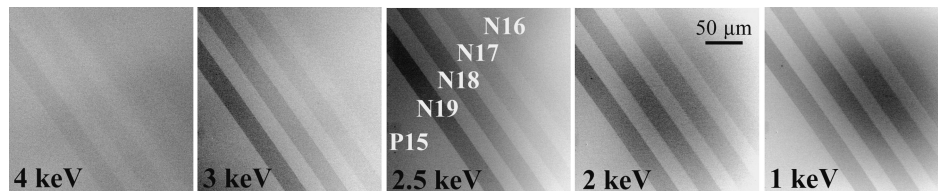


Fig. 5 Images of differently doped n-type stripes (N16 to N19) on the lightly doped p-type substrate (P15) obtained in the SLEEM device for various landing energies of the primary electron beam (indicated in the left bottom corner of the micrographs).

contrast. Around 1 keV the doping level dependency of the contrast weakens but the n-type and the p-type areas are still easy to distinguish.

Monte Carlo simulations of the BSE and the SE yields from silicon along the energy scale under examination have shown the BSE yield remaining nearly unchanged while the SE yield significantly increases with decreasing landing energy. With increasing landing energy the SE yield drops and later falls below that of the BSE so the dopant contrast decreases accordingly. At 1 keV the SE contribution dominates the total yield and fully determines the contrast appearance.

It follows that the contrast between the differently doped n-type areas and the p-type substrate is monotonically dependent on the doping level and the patterns can be clearly distinguished from the substrate in energy-filtered images. This is illustrated by the PEEM micrographs for various retarding voltages and also by the energy spectra. A part of the data was taken in the UHV SEM device with the landing beam energy in the low range of keV. The SE signal involves low energy electrons which should bear similar information as the photoelectrons detected in the threshold photoemission. The contrast behaviour in the SEM was found similar to the full photoemission signal obtained in the threshold PEEM.

An attempt to contribute to the contrast mechanism models in imaging of dopants in semiconductors might concentrate on differences in relations between n- and p-type spectra in threshold and core-level spectroscopies. The core-level spectra exhibit the same yields, which is in agreement with the generally small differences in the material composition. The spectrum shifts are proportional to the dopant concentration and show p-type photoemission at higher kinetic energies. This fact fits the assumption of at least partial Fermi level pinning, leaving some difference between ionization energies of the p- and the n-type with the former for the p-type being lower. Even with the full pinning, the subsurface field connected with band bending accelerates electrons toward the surface in the p-type and retards them in the n-type,¹⁶⁾ producing the observed effect at least qualitatively. The curvature of the band bending and hence the subsurface field grows with the dopant density so even the proportionality to the doping level is justified. However, the p/n shift of the threshold spectra is opposite, which indicates an additional effect surpassing the previous one as regards the p/n difference in kinetic energies. The dopant level independence of this shift indicates a possible explanation based on photoemission from the surface states, which does not move along the energy scale and contributes to the threshold

emission. Finally, the photoyield difference with much lower emission from the n-type cannot be explained by a cutoff of an internal energy distribution with the surface potential barrier of a different height because the lower yield exhibits a higher kinetic energy. Here it remains to consider the p/n difference in the absorption of hot electrons owing to generation of the electron/hole pairs, which explanation, however, requires considering the valence band emission.¹²⁾

4. Conclusions

Threshold photoemission measurements revealed that the contrast between the differently doped n-type patterns and the p-type substrate is monotonically dependent on the doping level. This allows quantification of the doping levels in n-type areas. The energy-filtered images showed a distinct contrast between n- and p-type areas throughout the dopant density scale. For the threshold photoemission, the shift between their respective energy spectra appears to be independent on the dopant concentration. In core-level photoemission of the heavily doped n-type patterns the shift between the spectra depends on the doping level and represents the source of contrast. Images taken in the ultra-high vacuum scanning electron microscope with the landing beam energy in the low range of keV showed behaviour of the contrast similar to the full threshold photoemission.

Acknowledgement

The work has been supported by the Czech Science Foundation project no. GP102/09/P543, by the Grant Agency of ASCR project no. IAA100650803 and by MSM T project no. MSM 0021622410. The authors are grateful to Mr M. Kucera (Faculty of Science, Masaryk University, Brno) for his help with samples production in the clean room laboratory of the Masaryk University, to Mr M. Libezny and Mr J. Petrovic (ON Semiconductor Czech Republic, Roznov pod Radhostem) for performing the ion implantation and spreading resistance profiling, to Mr F. Matejka (Institute of Scientific Instruments of the ASCR, Brno) for his advices concerning the sample production and preparation in general, and to Mr V. Kolarik (Institute of Scientific Instruments of the ASCR, Brno) for his help with preparation of the photolithography masks.

We acknowledge the ANKA Angstroemquelle Karlsruhe (Germany) for provision of the beamtime. All PEEM measurements were done at the WERA beamline and thanks are also due to the scientific staff at WERA, P. Nagel and S. Schuppler, for their interest and willingness to help.

REFERENCES

- 1) N. Duhayon *et al.*: *J. Vac. Sci. Technol. B* **22** (2004) 385–393.
- 2) S. L. Elliott, R. F. Broom and C. J. Humphreys: *J. Appl. Phys.* **91** (2002) 9116–9122.
- 3) P. Kazemian, S. A. M. Mentink, C. Rodenburg and C. J. Humphreys: *J. Appl. Phys.* **100** (2006) 054901, 1–7.
- 4) I. Müllerová, M. M. El-Gomati and L. Frank: *Ultramicroscopy* **93** (2002) 223–243.
- 5) C. G. H. Walker, F. Zaggout and M. M. El-Gomati: *J. Appl. Phys.* **104** (2008) 123713, 1–6.
- 6) V. W. Ballarotto, K. Siegrist, R. J. Phaneuf, E. D. Williams and S. Mogren: *Surf. Sci.* **461** (2000) L570–L574.
- 7) V. W. Ballarotto, K. Siegrist, R. J. Phaneuf and E. D. Williams: *J. Appl. Phys.* **91** (2002) 469–475.
- 8) R. J. Phaneuf, H.-C. Kan, M. Marsi, L. Gregoratti, S. Günther and M. Kiskinova: *J. Appl. Phys.* **88** (2000) 863–868.
- 9) M. Hovorka, L. Frank, D. Valdaitsev, S. A. Nepijko, H. J. Elmers and G. Schönhense: *J. Microsc.* **230** (2008) 42–47.
- 10) M. Merkel, M. Escher, J. Settemeyer, D. Funnemann, A. Oelsner, Ch. Ziethen, O. Schmidt, M. Klais and G. Schönhense: *Surf. Sci.* **480** (2001) 196–202.
- 11) I. Müllerová and L. Frank: *Adv. Imaging Electron Phys.* **128** (2003) 309–443.
- 12) L. Frank, I. Müllerová, D. Valdaitsev, A. Gloskovskii, S. A. Nepijko, H. J. Elmers and G. Schönhense: *J. Appl. Phys.* **100** (2006) 093712, 1–5.
- 13) F. J. Himpsel, F. R. McFeely, A. Taleb-Ibrahimi, J. A. Yarmoff and G. Hollinger: *Phys. Rev. B* **38** (1988) 6084–6096.
- 14) R. Schlaf, R. Hinogami, M. Fujitani, S. Yae and Y. Nakato: *J. Vac. Sci. Technol. A* **17** (1999) 164–169.
- 15) S. Iwata and A. Ishizaka: *J. Appl. Phys.* **79** (1996) 6653–6713.
- 16) M. M. El-Gomati, T. C. R. Wells, I. Müllerová, L. Frank and H. Jayakody: *IEEE Trans. Electron Devices* **51** (2004) 288–291.